Rayleigh Fiber Optics Gyroscope

A. Küng, J. Budin, L. Thévenaz, and Ph. A. Robert, *Member, IEEE*

***Abstract*— A novel kind of fiber-optic gyroscope based on Rayleigh backscattering in a fiber-ring resonator is presented in this letter. The information on the rotation rate is obtained from the composed response of the fiber ring to an optical time-domain reflectometry (OTDR) instrument. The developed model based on the coherence properties of the Rayleigh scattering yields to a polarization-insensitive and low-cost gyroscope.**

***Index Terms*— Gyroscope, optical fiber devices, optical fiber interference, optical fiber scattering, optical time domain reflectometer (OTDR), Rayleigh scattering, time-domain measurements.**

I. Introduction

SINCE detection of rotation with light was demonstrated by Sagnac [1] in 1913 the increased effort over these past few years leads to classify fiber-optic gyroscopes (FOG's) among one of the following three working criteria: interferometric FOG [2], resonant FOG [3], or Brillouin FOG [4]. However, this letter presents a novel type of FOG based on Rayleigh backscattering in a fiber ring resonator that cannot be simply classified among those criteria. The aim of studying such astonishing gyroscope is not to reach high-grade performances but to built low-cost and polarization insensitive fiber-optic gyros and moreover to understand the unique behavior of Rayleigh backscattering in a fiber-ring configuration that can limit Resonant and Brillouin FOG's sensitivity.

The idea of using an optical time-domain reflectometry (OTDR) instrument to interrogate a fiber-optic ring resonator was originally developed for characterizing fiber ring resonators [5]. The ring structure has the unique feature to let the OTDR pulse circulate many times in the ring while generating Rayleigh backscattering. This recirculation of the OTDR pulse combined together with the re-circulation of the Rayleigh backscattered light allows different Rayleigh contributions to be detected simultaneously resulting in a step-like OTDR trace, as shown in Fig. 1. The first steps are given by few contributions of great intensity. As the step order is getting higher the number of contributions grows and their intensity decays resulting in a maximum. The relevant ring parameters can be extracted by simply measuring the position of this maximum [5]. But rotation of the fiber ring also affects the OTDR trace as shown in Fig. 2 for increasing rotation rates. This sensitivity to the Sagnac effect can only be explained considering that some of the different Rayleigh contributions are mutually coherent [6]. Multiple recirculation of low-coherent light in a ring resonator has been studied in the case of a external reflective end [7], but not in this specific time-dependent case of Rayleigh backscattered light distributed all along the fiber ring.

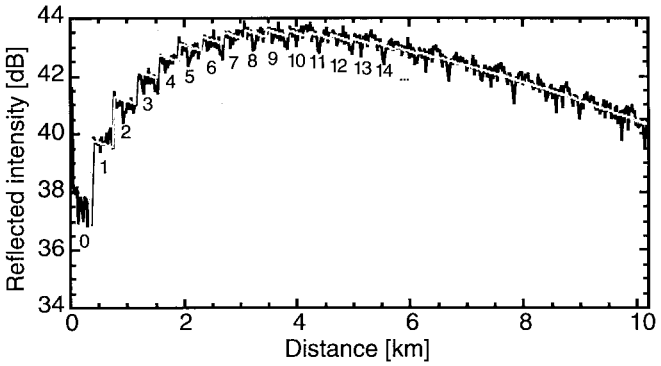

Fig. 1. OTDR trace of a 765-m-long fiber ring resonator at rest with a coupler coefficient $k = 95\%$ and numerical fit of (7), giving a calculated cavity feedback [5] coefficient $k_r = 89.5\%$. The first step orders are indicated.

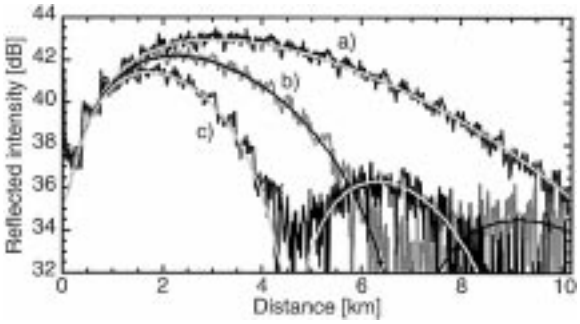

Fig. 2. OTDR traces of the same 765-m-long fiber ring resonator with respective numerical fit of (8) for rotation rates: (a) 0.1 rad/s, (b) 0.2 rad/s, and (c) 0.3 rad/s.

Model of Rayleigh backscattering in a fiber ring including the Sagnac effect will be described in the first part of this letter. Then measurements performed on a 765-m ring made of standard single-mode fiber will confirm the validity of the developed model. Finally, performances of such a gyro will be discussed.

The model of the intensity Rayleigh backscattered signal is obtained by considering the Rayleigh backscattered contributions generated in the ring by a coherent probe pulse uniformly scattered while circulating along the fiber ring in the counterclockwise direction, as described in Fig. 3. The backscattered light also circulates in the ring but in the clockwise direction and part of it is directed onto the OTDR detection stage at each turn.

The traces are, thus, made of equal length steps corresponding to the ring length. Each step results from the addition

Manuscript received February 12, 1997; revised April 2, 1997.

The authors are with the Swiss Federal Institute of Technology (EPFL), Laboratory of Metrology, CH-1015 Lausanne, Switzerland.

Publisher Item Identifier S 1041-1135(97)05045-3.

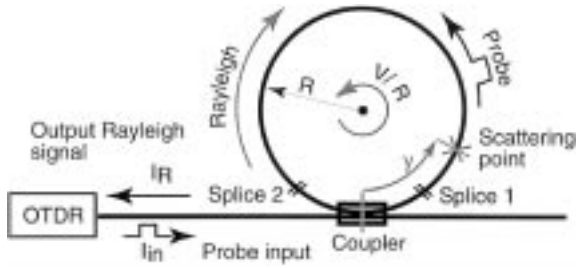

Fig. 3. Schematic description of a Rayleigh fiber ring gyroscope of radius R, rotating at angular speed v/R.

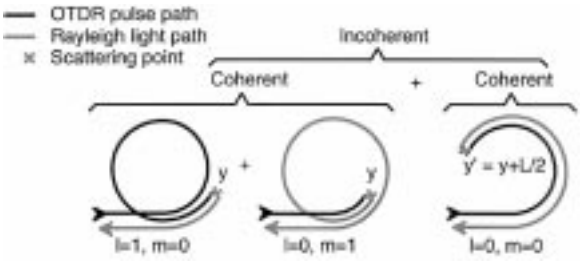

Fig. 4. Addition of the 3 contributions of step 1. The contributions scattered at the same point are added coherently.

of a definite number of contributions circulating in the ring at the given propagation time. But only the contributions which were detected *simultaneously* and scattered by the *same scattering point* are mutually coherent and interfering [6], making the signal envelope shape strongly dependent on the differential propagation phase of all these contributions. The chosen referential is fixed to the rotating ring, so that the probe pulse and Rayleigh light experience different speeds (c_p and c_r, respectively) which are determined by velocity addition according to special relativity

$$c_p = \frac{c_0}{n} - \chi v \tag{1}$$

$$c_r = \frac{c_0}{n} + \chi v \tag{2}$$

$$\chi = 1 - \frac{1}{n^2} \tag{3}$$

where χ is the Fizeau drag first-order correction factor [8], c_0 is the vacuum velocity of light, n is the propagation refractive index through the ring at rest, and v is the ring tangential speed (v is chosen positive in the probe direction).

The electric field resulting from the OTDR probe pulse which made l turns (counterclockwise) in the ring at velocity c_p, being scattered at a distance y from the coupler and which made m turns back (clockwise) at velocity c_r is given by

$$E_{lm}(y) = E_{00}(y)(k\xi)^{(l+m)/2} \exp\left[-\frac{\alpha}{2}(l+m)L\right] \times \exp\{i\beta L[(l+m) + \chi v^{n/c_0}(l-m)]\} \tag{4}$$

where $E_{00}(y)$ represents the electric field amplitude for $l = m = 0$:

$$E_{00}(y) = \sqrt{I_{\text{in}} R(y)}\,(1-k)\xi \exp(-\alpha y) \exp(i2\beta y) \tag{5}$$

where I_{in} is the input intensity, β is the propagation constant, k the intensity coupling coefficient of the coupler, ξ is the intensity transmission coefficient of the ring excluding the fiber linear loss, $R(y)$ is the intensity Rayleigh backscattering coefficient, α is the intensity linear attenuation of the fiber, L is the ring length and $y (0 \le y \le L)$ is the distance along the fiber from the coupler to the scattering point.

To obtain the electric field (4) the following first-order approximation has been made:

$$(c_0 - v)(c_0 + v) \cong c_0^2. \tag{6}$$

The ring resonators used for Rayleigh backscattering gyros are preferably several hundred meters long to enhance the Sagnac phase shift due to the ring rotation. It has been formally demonstrated in [5] that such long ring resonators present negligible polarization sensitivity and, therefore, polarization problems are not taken into account in this description.

The resulting OTDR trace is obtained by summing over l and m each contribution given in (4) which experienced the same propagation time. As these contributions are generated simultaneously by the same source and also detected simultaneously they must be added coherently. However, as a result of the random character of Rayleigh backscattering, the contributions scattered from different scattering centers are not correlated [6] and must be added incoherently. For a given propagation time, each contribution is scattered only by either of the two different centers spaced by a distance $L/2$ as described in Fig. 4 for step number 1.

These considerations lead to the following discontinuous step-like model of the backscattered intensity signal given by the OTDR:

$$I_u(y) = I_0(y)(k\xi)^{u-1} \exp(-\alpha u L) \times \left\{ k\xi \left| \sum_{p=0}^{u} \exp\left[i\beta L \frac{n}{c_0} \chi v (2p-u) \right] \right|^2 + \left| \sum_{p=0}^{u-1} \exp\left[i\beta L \frac{n}{c_0} \chi v (2p-u+1) \right] \right|^2 \right\} \tag{7}$$

where $I_0(y) = |E_{00}(y)|^2$ corresponds to the intensity function for step zero, the integer $u = \text{int}(z/L)$ is the step order and z is the total propagation distance. The position $y\,(0 \le y \le L/2)$ of the scattering center is simply related to the total distance by $z = uL + 2y$.

The summations contained in the discontinuous backscattered intensity function (7) can be replaced by the corresponding integral resulting in a continuous function:

$$I(u) = I_{in} R(u) \xi^2 (k\xi)^{u-1} \exp\left[-\alpha L\left(u + \tfrac{1}{2}\right)\right] \times \frac{\left\{ k\xi \sin^2\left[\beta L \frac{n}{c_0} \chi v (u+1) \right] + \sin^2\left(\beta L \frac{n}{c_0} \chi v u \right) \right\}}{\left(\beta L \frac{n}{c_0} \chi v \right)^2} \tag{8}$$

where u is now a continuous parameter:

$$u = \frac{z}{L} - \frac{1}{2} \tag{9}$$

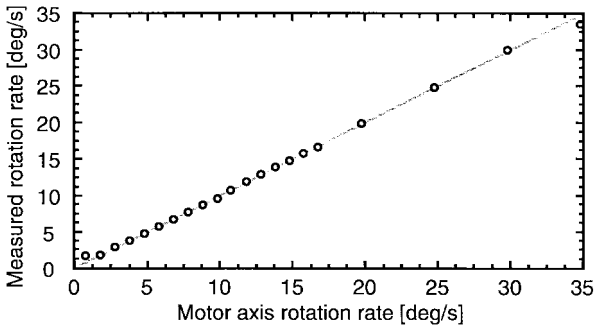

Fig. 5. Measured rotation rate using fitting of expression (8) as a function of the actual rotation rate.

Thus, if the ring parameters k, L, α, n, and ξ are known, the rotation rate can be determined through an easy signal processing by fitting (8) over the OTDR signal. It turns out that this relation is an even function of v indicating that the gyroscope in this simple configuration is insensitive to the rotation direction.

The tangential velocity v and the ring length L are closely related through the ring geometry, so that the Sagnac phase shift responsible for the gyro sensitivity is proportional to the total area enclosed by the fiber loop like in any other I-FOG. Nevertheless, increasing the length of the fiber also increases the intracavity loss resulting in a steeper final slope of the OTDR signal, and a reduced sensitivity, accordingly.

Measurements were performed on a long ring gyroscope made of 765 m of single-mode fiber spliced to a 5/95% coupler and wound on a 14-cm diameter drum. The OTDR traces were obtained with no time averaging from a commercial instrument having a 10-nm-wide spectra at 1310 nm. Fig. 2 shows the fitting of (8) on the OTDR traces obtained for different rotation rates. In our experiment this gyroscope was mounted on the axis of a stepping motor. The rotation rate measured by the gyroscope is in excellent agreement with the rotation rate of the motor axis, as shown in Fig. 5.

At low-rotation rates the OTDR trace is only significantly affected after many circulations in the ring (long distances) resulting in an increase of the signal final slope. Slow rotation detection and resolution are thus limited by the OTDR signal noise that makes two curves measured at very close rotation rates indistinguishable. The obtained resolution of our experimental gyroscope was 0.01 rad/s without any averaging. As the rotation rate increases the final slope first becomes steeper and then other minimas and maximas appear periodically at the end of the OTDR trace (Fig. 2). For sufficient high-rotation rates the signal periodicity and the step length become comparable. The signal is then under-sampled by the ring steps and approximation made in (8) is no longer valid. To overcome this limitation, fitting of the discontinuous relation in (7) is then required.

A novel kind of fiber-optic gyroscope based on Rayleigh backscattering in a fiber-optic ring resonator is reported. The information on the rotation rate is extracted from the typical response of the fiber ring to an optical time-domain reflectometry (OTDR) instrument. The developed model based on the coherence properties of the Rayleigh scattering yields to a polarization-insensitive gyroscope. Surprisingly good performances are achieved by this easy-to-built and low-cost fiber-optic gyroscope.

REFERENCES

[1] G. Sagnac, "L'éther lumineux démontré par l'effet du vent relatif d'éther dans un interféromètre en rotation unifome," *Compte rendus de l'Acadmie des Sciences*, vol. 95, pp. 708–710 and 1410–1413, 1913.
[2] R. A. Bergh, H.C. Lefvre, and H. J. Shaw, "All-single-mode fiber-optic gyroscope," *Opt. Lett.*, vol. 6, no. 4, pp. 198–200, 1981.
[3] K. Iwatsuki, K. Hotate, and M. Higashiguchi, "Backscattering in an optical passive ring-resonator gyro: Experiment," *Appl. Opt.*, vol. 25, no. 23, pp. 4448–4451, 1986.
[4] S. P. Smith, F. Zarimetchi, and S. Ezekiel, "Narrow-linewidth stimulated Brillouin fiber laser and applications," *Opt. Lett.*, vol. 16, no. 6, pp. 393–395, 1991.
[5] A. Küng, J. Budin, L. Thévenaz, and P. A. Robert, "Optical fiber ring resonator characterisation by optical time-domain reflectometry," *Opt. Lett.*, vol. 22, vo. 2, pp. 90–92, 1997.
[6] P. Gysel and R. K. Staubli, "Statstical properties of Rayleigh backscattering in single-mode fiber," *J. Lightwave Technol.*, vol. 8, pp. 561–567, Apr. 1990.
[7] I. P. Giles, M. Farhadiroushan, and R. C. Youngquist, "Low coherence resonant ring rotation sensor," in *Proc. 4th Int. Conf. Optical Fiber Sensors (OFS'86)*, Tokyo, Japan, 1986, pp. 205-208.
[8] H. Lefvre, *The Fiber-Optic Gyroscope*. Norwood, MA: Artech House, 1993, p. 11.